Variation in the Absolute Photonic Band Gap of Rods Ranging from Square to Octagonal in Square Lattices



2011 Jpn. J. Appl. Phys. 50 072002

(http://iopscience.iop.org/1347-4065/50/7R/072002)

Japanese Journal of Applied Physics **50** (2011) 072002 **REGULAR PAPER**
**DOI:** 10.1143/JJAP.50.072002

# Variation in the Absolute Photonic Band Gap of Rods Ranging from Square to Octagonal in Square Lattices

Chung-An Hu[1], Kuo-Pin Chang[1], Su-Lin Yang[1]*, Lin Fang Shen[2], Jin-Jei Wu[3], and Tzong-Jer Yang[1,3]

[1]*Department of Electrophysics, National Chiao Tung University, Hsinchu 30050, Taiwan, Republic of China*
[2]*Electromagnetic Academy, Zijingang Campus, Zhejiang University, Hangzhou 310058, People's Republic of China*
[3]*Department of Electrical Engineering, Chung Hua University, Hsinchu 30012, Taiwan, Republic of China*

Received March 25, 2011; revised April 30, 2011; accepted May 10, 2011; published online July 20, 2011

The band structures and field patterns of dielectric rods in square lattices are calculated using the plane-wave method. The rods with various cross-sectional shapes from square to octagonal at a fixed filling-factor are constructed to assess the geometry effect of photonic crystals to their band gap properties. Analytical results indicate that the corner profiles of rods significantly affect the *E*- and *H*-polarization bands in resonance frequency and field distribution. The absolute photonic band gap is closed in the square lattice when square dielectric rods are replaced with octagonal dielectric rods. 

## 1. Introduction

Periodic dielectric structures (photonic crystals) have garnered considerable interest in the recent decade owing to their ability to prohibit certain frequency-ranged electromagnetic (EM) waves from propagating in such structured dielectric media.[1–3] These frequency regions are called photonic band gaps (PBGs), and are analogous to electronic band gaps resulting from periodic electrostatic potentials in crystals. The polarization-independent PBGs, called absolute PBGs, occur when the band gaps of both *H*- and *E*-polarization modes overlap. Absolute PBGs can control spontaneous light emissions for non-threshold semiconductor lasers.[4,5]

The fabrication and simulation of photonic crystals in the infrared (IR), ultraviolet (UV), and visible regions have received considerable interest.[6–11] However, the greatest constraint to large PBG width is the degeneration of photonic bands at the highly symmetrical points in the Brillouin zone. Several approaches have been developed to reduce band degradation to obtain large absolute PBGs, which requires varying the contrast of the dielectric contrast ratio, designing the lattice element, tuning the filling ratio and reducing structural symmetries.[12–17] As a rule of thumb, the formation of band gaps in a photonic crystal is attributed to the arrangement of connected veins and the isolated dielectric material.[18–20] This observation suggests that isolated high-dielectric regions are favorable for large *E*-polarized band gaps, while connected veins are favorable for large *H*-polarized band gaps. Thus, an absolute PBG should be favored in photonic crystals with highly dielectric regions that are both isolated and connected.

As is well known, although appearing in a square lattice when square dielectric rods are used, the absolute PBG vanishes when these square rods are replaced with circular or hexagonal dielectric rods.[21,22] However, how this variation occurs has not been examined. This study first demonstrates that using octagonal rods in a square lattice cannot open absolute PBGs. Why such distinct outcomes exist from square and octagonal rods in a square lattice is an interesting question. The shape and boundary of rods may markedly influence band structure. To elucidate how rod shape and boundary affect PBG formation in a square lattice, this study reshapes the corners of initial square rods gradually, forming all the way to octagonal rods with a fixed filling factor. Band structures and field patterns are estimated using the plane-wave method. The effects of rod shape on *E*- and *H*-polarization modes are then determined. Additionally, the center and width of bands associated with the absolute PBG of square dielectric rods in a square lattice are calculated.

## 2. Theory

The photonic band gap can be obtained by solving Maxwell's equations. Assume a source free, time-invariant, and nonpermeable ($\mu = \mu_0$) space; thus, Maxwell's equations can be written in terms of magnetic field $\mathbf{H}$ as a master equation,

$$\nabla \times \left[\frac{1}{\varepsilon(\mathbf{r})} \nabla \times \mathbf{H}(\mathbf{r})\right] = \frac{\omega^2}{c^2}\mathbf{H}(\mathbf{r}), \tag{1}$$

where $\mathbf{H}(\mathbf{r})$ is the magnetic field, $\varepsilon(\mathbf{r})$ is a position-dependent dielectric constant, $\omega$ is angular frequency, and $c$ is the speed of light in a vacuum. For a periodic system, the magnetic field, $\mathbf{H}(\mathbf{r})$, and dielectric function, $\varepsilon(\mathbf{r})$, can be expressed as sums of plane waves:

$$\mathbf{H}(\mathbf{r}) = \sum_{\mathbf{G}} \sum_{\lambda=1,2} h_{\mathbf{G},\lambda} \hat{e}_\lambda e^{i(\mathbf{k}+\mathbf{G})\cdot\mathbf{r}}, \tag{2}$$

$$\varepsilon(\mathbf{r}) = \sum_{\mathbf{G}} \varepsilon(\mathbf{G}) e^{i\mathbf{G}\cdot\mathbf{r}}, \tag{3}$$

where $h_{\mathbf{G},\lambda}$ is a coefficient of the $\mathbf{H}$ component, $\mathbf{k}$ is the wave vector in the Brillouin zone, and $\mathbf{G}$ is the reciprocal-lattice vector. Two independent polarizations characterized by unit vectors $\hat{e}_\lambda(\lambda = 1, 2)$ are perpendicular to the propagation vector $(\mathbf{k} + \mathbf{G})$. Under the Fourier transform, the coefficient of $\varepsilon(\mathbf{G})$ is defined as

$$\varepsilon(\mathbf{G}) = \frac{1}{A_{\text{cell}}} \int_{\text{cell}} \varepsilon(\mathbf{r}) e^{-i\mathbf{G}\cdot\mathbf{r}}\, dr, \tag{4}$$

where $A_{\text{cell}}$ is the area of a primitive lattice cell. Thus, eq. (1) can be expressed in a matrix form as

*E-mail address: slyang@mail.nctu.edu.tw

 

$$\sum_{G'} |\mathbf{k}+\mathbf{G}||\mathbf{k}+\mathbf{G}'| \begin{bmatrix} \hat{e}_2 \cdot \varepsilon^{-1}_{\mathbf{G},\mathbf{G}'} \cdot \hat{e}_2{}' & -\hat{e}_2 \cdot \varepsilon^{-1}_{\mathbf{G},\mathbf{G}'} \cdot \hat{e}_1{}' \\ -\hat{e}_1 \cdot \varepsilon^{-1}_{\mathbf{G},\mathbf{G}'} \cdot \hat{e}_2{}' & \hat{e}_1 \cdot \varepsilon^{-1}_{\mathbf{G},\mathbf{G}'} \cdot \hat{e}_1{}' \end{bmatrix} \begin{bmatrix} h_{1,\mathbf{G}'} \\ h_{2,\mathbf{G}'} \end{bmatrix} = \frac{\omega^2}{c^2} \begin{bmatrix} h_{1,\mathbf{G}} \\ h_{2,\mathbf{G}} \end{bmatrix}, \tag{5}$$

where $\varepsilon^{-1}_{\mathbf{G},\mathbf{G}'} = \varepsilon^{-1}(\mathbf{G}-\mathbf{G}')$ is the inverse of matrix $\varepsilon(\mathbf{G}-\mathbf{G}')$. The eigenvalue equation, eq. (5), can then be solved using the matrix diagonalization method.

For a two-dimensional (2D) photonic crystal, an electromagnetic (EM) wave can be decomposed into $E$-polarized (the electrical field is parallel to the $z$-axis) and $H$-polarized (the magnetic field is parallel to the $z$-axis) modes. Calculations are restricted to the case in which wave vectors of eigenmodes are on the 2D $x$–$y$ plane and are uniform in the $z$-direction. The dielectric constant is given by

$$\varepsilon(\mathbf{G}) = \begin{cases} \varepsilon_a \cdot f + \varepsilon_b \cdot (1-f) & \text{for } \mathbf{G}=0 \\ (\varepsilon_a - \varepsilon_b) \cdot S(\mathbf{G}) & \text{for } \mathbf{G} \neq 0 \end{cases}, \tag{6}$$

where $\varepsilon_a$ and $\varepsilon_b$ are the dielectric constants of rods and the background medium, respectively. Filling factor $f$ is the cross-sectional area fraction of rods in a primitive unit cell. The structure factor is denoted by

$$S(\mathbf{G}) = \frac{1}{A_{\text{cell}}} \int_{\text{Rod}} e^{-i\mathbf{G}\cdot\mathbf{r}}\, dr. \tag{7}$$

Here, the integral is over the cross section of rods in a unit cell of the lattice. In this study, the structural factor for each corner-cutting structure can be derived from polygonal rod concepts. For a polygonal rod, this study considers a polygonal rod with $N$ sides; the coordinate of the $j$th vertex is denoted by $\mathbf{P}_j = (x_j, y_j)$. According to the Stokes theorem, the structural factor for a polygonal rod can be written as

$$S(\mathbf{G}) = \begin{cases} \displaystyle\sum_{j=1}^{N} \frac{i\Delta y_j e^{-i\mathbf{G}\cdot\mathbf{C}_j}}{G_x} \frac{\sin(\mathbf{G}\cdot\mathbf{S}_j)}{\mathbf{G}\cdot\mathbf{S}_j} & \text{for } G_y = 0 \\ \displaystyle\sum_{j=1}^{N} \frac{-i\Delta x_j e^{-i\mathbf{G}\cdot\mathbf{C}_j}}{G_y} \frac{\sin(\mathbf{G}\cdot\mathbf{S}_j)}{\mathbf{G}\cdot\mathbf{S}_j} & \text{for } G_x = 0 \\ \displaystyle\sum_{j=1}^{N} \frac{2i\hat{e}_z(\mathbf{G}\cdot\mathbf{S}_j) e^{-i\mathbf{G}\cdot\mathbf{C}_j}}{G^2} \frac{\sin(\mathbf{G}\cdot\mathbf{S}_j)}{\mathbf{G}\cdot\mathbf{S}_j} & \text{for } G_x \neq 0, G_y \neq 0 \end{cases}, \tag{8}$$

with

$$\mathbf{C}_j \equiv \left(\frac{\mathbf{P}_{j+1} + \mathbf{P}_j}{2}\right),$$
$$\mathbf{S}_j \equiv \left(\frac{\mathbf{P}_{j+1} - \mathbf{P}_j}{2}\right),$$
$$\Delta x \equiv x_{j+1} - x_j,$$
$$\Delta y \equiv y_{j+1} - y_j.$$

The band structures for a photonic crystal are calculated using the standard plane-wave method. In this study, 841 plane waves were adopted, and computational errors in the $E$- and $H$-polarized modes for each structure were estimated at $<1\%$.

## 3. Results and Discussion

Figure 1 shows the cross-sectional geometry of the octagonal rod formed by cutting the corners of a square rod. The lengths of the cut-corner edge and rod central side are designated as $b$ and $l$, respectively. Each photonic crystal with exact, inexact octagonal, or square rods has the same optimal filling factor of $f = 0.45$. The difference in the size of the cut corner edge between the exact octagonal rod and square rod is $l_8/\sqrt{2}$, where $l_8$ is the side length of the exact octagonal rod. The dielectric constant of the rod is $\varepsilon_a = 12.96$, corresponding to that of gallium arsenide (GaAs) or silicon at 1.55 μm, and the dielectric constant for the background material is taken as $\varepsilon_b = 1$ for air or the vacuum. In this study, the corners are cut from the square rod to generate an octagon by 15 steps with an increment of $\beta = l_8/(15 \cdot \sqrt{2})$. For convenience, the size of cut corner edge is denoted as $b = N \cdot \beta$, for $N = 0, 1, \ldots, 14, 15$.

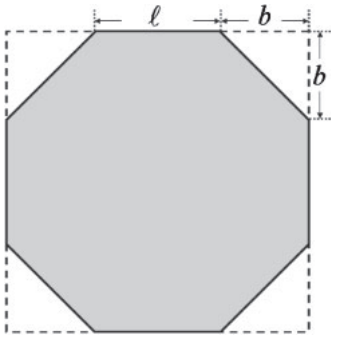


**Fig. 1.** Representation and cross-sectional geometry of rods.

Figures 2(a) and 2(b) show the photonic band structures associated with the square rods ($b = 0 \cdot \beta$) and octagonal rods ($b = 15 \cdot \beta$) in square lattices, respectively, with a filling factor $f = 0.45$. In Fig. 2, the solid curves represent $E$-polarized modes and dotted curves represent $H$-polarized modes. The dispersion curves are traced along the $T$–$X$–$M$–$T$ path in the first Brillouin zone of square lattices. The square dielectric rods in square lattices generate an absolute PBG occurring where the $E_8$ and $H_6$ gaps overlap, where $E_i$ or $H_i$ is the gap between the $i$th and $(i+1)$th bands for the corresponding polarizations [Fig. 2(a)]. The absolute gap center is at $0.628(\omega a/2\pi c)$ and the absolute PBG width is $0.036(\omega a/2\pi c)$. Conversely, the absolute PBG closes when the square dielectric rods are replaced with octagonal dielectric rods [Fig. 2(b)], suggesting that the four corners of square rods may markedly influence band structure.

To determine why such a difference exists in appearance of the absolute PBG between square rods and octagonal rods in the square lattice, the corners of square rods were cut to form an octagonal rod gradually while the filling factor remained constant. Figure 3 shows the dependence of the gap map on the cutting step $N$. Here this study only considers the frequency range of interest of $0.55 \sim 0.7(\omega a/2\pi c)$. Analytical results indicate that the widths of $E_8$ and $H_6$ gaps decline simultaneously as $N$ increases. The variation in frequencies of air bands ($E_9$ and $H_7$ bands) is larger than that of dielectric bands ($E_8$ and $H_6$ bands), and thus dramatically reduces absolute band gap width.

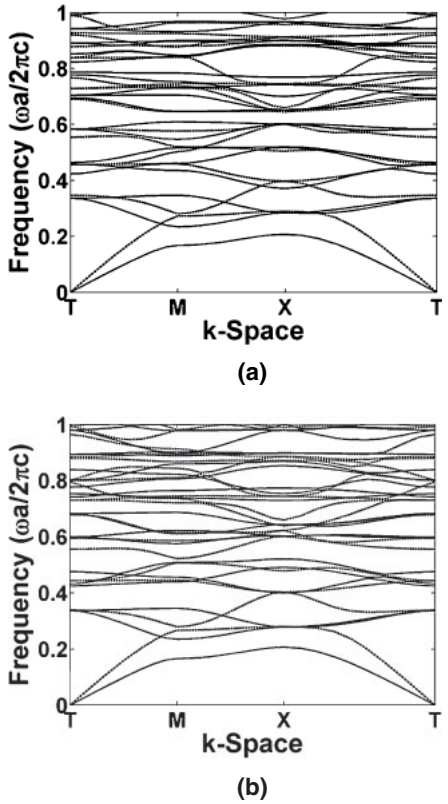


**Fig. 2.** Photonic band structures for (a) square rods ($b = 0$) and (b) octagonal rods ($15 \cdot \beta$) in the square lattice with a filling factor of 0.45.

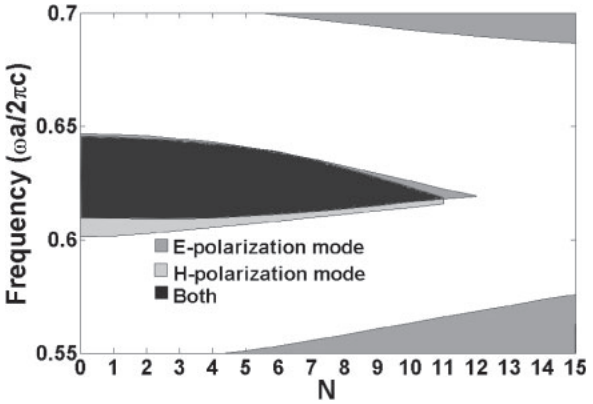


**Fig. 3.** The gap map as a function of $N$. The corresponding size of cutting edges for each structure is $N \cdot \beta$.

To examine the effect of cutting the edges on $E$-polarization modes, Figs. 4(a)–4(d) plot the field patterns for structures of $N = 0$, 8, 11, and 15, respectively. At the $M$-symmetrical point, field patterns of each figure are displayed for the $E_8$ (left) and $E_9$ (right) bands. The field distributions of the $E_8$ band are generally independent of $N$; however, the amounts of field energy inside rods increase as $N$ increases. For field patterns of the $E_9$ band, the shape of rods strongly affects the field distribution and the amount of field energy. When $N$ increases, the fields near the boundary of a rod are expelled from dielectric regions and the amount of field energy decreases. Because the amount of field energy inside dielectric rods is closely related to band frequency, the difference in the amount of field energy between $E_8$ and $E_9$ bands may lead to the absence of the $E$-polarized gap.

The perspective of the band structure is adopted to understand why the absolute PBG appears in square rods, but is disappear in octagonal rods. For a given band, the band center (BC) reflects the resonant frequency of modes, while band width (BW) reflects the strength of the interaction of EM waves among rods. These band-structure concepts are similar to those in the A linear combination of atomic orbitals (LCAO) method.[23–25] Here, the BC and BW are defined as

$$F_i(\mathrm{BC}) = \frac{F_{i,\max} + F_{i,\min}}{2}, \qquad F_i(\mathrm{BW}) = F_{i,\max} - F_{i,\min} \tag{9}$$

where $F_{i,\max}$ and $F_{i,\min}$ denote the maximum and minimum frequencies of the $i$th band in the first Brillouin zone, respectively. Here, the $E$- and $H$-polarized bands associated with the absolute PBG in the photonic crystal are utilized. Figures 5(a) and 5(b) show the BC and BW of the $E_8$ and $E_9$ bands as a function of $N$, respectively. The BC of the $E_9$ band varies faster than that of $E_8$ band when $N$ exceeds 4. These analytical results demonstrate that the effect of the cutting edge on the resonance frequency of the $E_9$ band is stronger than that on the $E_8$ band, and the resonance frequencies for both bands gradually approach each other and move closer as $N$ increases. Furthermore, this study examines BW to investigate how field energy concentrates inside dielectric regions and influences band structures. The BW of the $E_9$ band when $N$ increases is markedly different than that of the $E_8$ band. The BW for the $E_8$ band is almost independent of $N$, implying that field energies are localized in the dielectric rods. However, the BW of the $E_9$ band exhibits a large variation and increases to 137% at $N = 11$. These analytical results likely indicate that the partial fields of the $E_9$ band are expelled from the dielectric rods when the cutting edge of the rod changes. Although the BC and BW of the $E_8$ band are insensitive to the shape or boundary of rods, the BC decreases and BW increases for the $E_9$ band close the $E$-polarized gap when $N$ exceeds 11.

Figures 6(a) and 6(b) show the BC and BW associated with the $H_6$ and $H_7$ bands varying with $N$. The BC of the $H_6$ band varies slightly with $N$; however, the BC of the $H_7$ band varies markedly, indicating that the resonance frequency of $H_7$ band depends strongly on rod shape. Moreover, the BWs for both $H_6$ and $H_7$ bands have large variations with $N$ and both increase by roughly 0.017 when $N = 11$. Thus, the fields propagated in the $x$–$y$ plane cannot be localized well inside the dielectric region when the cut edge of the rod changes. Notably, the fields of the $H$-polarization modes concentrated in the rods are closely related to the air-space size among the rods.[13] This study fixes the filling factor throughout calculations, and the air-space size among rods consequently varies with $N$. Therefore, both bands have the same BW increment is acceptable. Because of the decrease in resonance frequency of the $H_7$ band and increase in BWs for both the $H_6$ and $H_7$ bands, the $H$-polarized gap may close.

## 4. Conclusions

Exactly why the absolute PBG appears in square rods but closes in octagonal rods is investigated from the aspect of

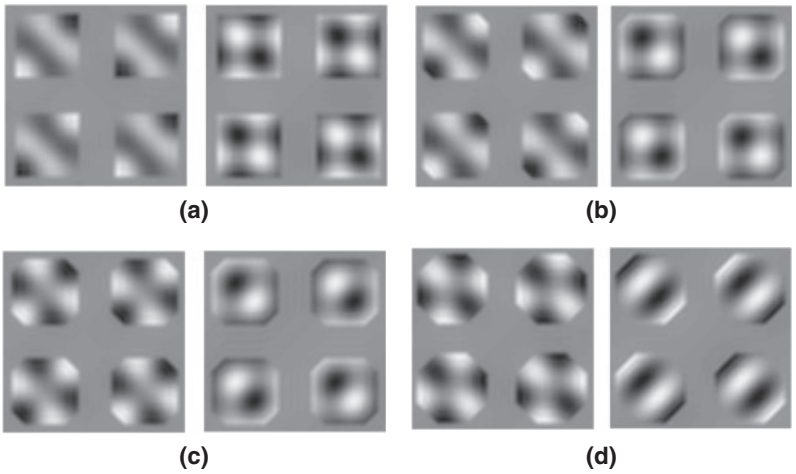


**Fig. 4.** Field patterns of $E$-polarized modes inside dielectric rods when (a) $N = 0$, (b) $N = 8$, (c) $N = 10$, and (d) $N = 15$, for the $E_8$ band and at the $M$-symmetrical point.

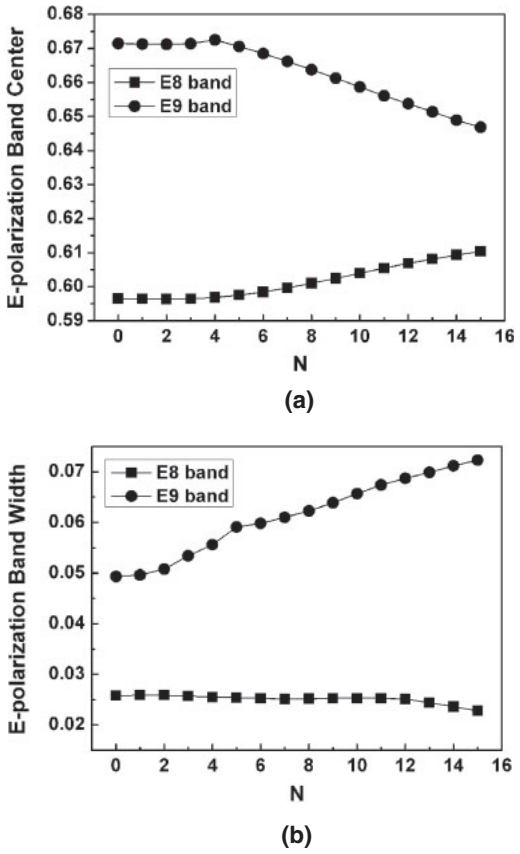


**Fig. 5.** (a) Band center and (b) band width associated with the $E_8$ and $E_9$ bands as a function of $N$.

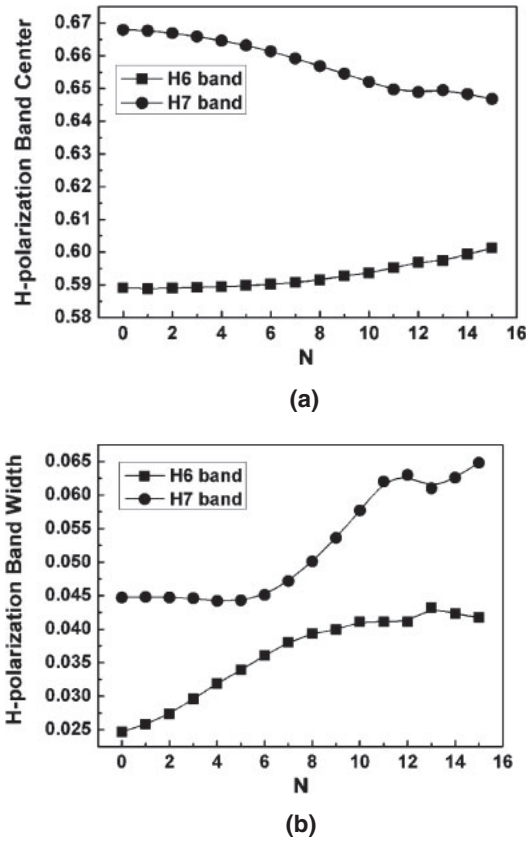


**Fig. 6.** (a) Band center and (b) band width associated with the $H_6$ and $H_7$ bands as a function of $N$.

band structure and field patterns. The perspective of band structure is helpful in understanding the formation of the PBG in photonic crystals. This study employed the plane-wave method to calculate band structures and field patterns. The corners of square rods were changed step by step to fabricate octagonal rods with a fixed filling factor throughout calculations. Analytical results for the $E$-polarized gap ($E_8$ gap) indicate that the cutting edges of rods strongly affect the $E_9$ band in the resonance frequency and field distribution inside rods. The decrease in resonance frequency and increase in band width caused the $E$-polarized gap to close. Moreover, the $H$-polarized gap ($H_6$ gap) was closely related to the cutting edges of rods. The decrease in resonance frequency of the $H_7$ band and increase in bandwidths of both $H_6$ and $H_7$ bands caused the $H$-polarized gap to close. Accordingly, the absolute PBG is closed in the square lattice when square dielectric rods are replaced with octagonal dielectric rods.

## Acknowledgments

The authors would like to thank the National Science Council of the Republic of China, Taiwan (Contract No. NSC-98-2112-M-009-019-MY2 and NSC-98-2112-M-216-001), and the National Science Foundation of China (Contract No. 60531020) for financially supporting this research.

1) E. Yablonovitch: Phys. Rev. Lett. **58** (1987) 2059.
2) S. John: Phys. Rev. Lett. **58** (1987) 2486.
3) E. Yablonovitch and T. J. Gmitter: Phys. Rev. Lett. **63** (1989) 1950.
4) W. D. Zhou, J. Sabarinathan, P. Bhattacharya, B. Kochman, E. W. Berg, P.-C. Yu, and S. W. Pang: IEEE J. Quantum Electron. **37** (2001) 1153.
5) K. Inoue, M. Sasada, J. Kawamata, K. Sakoda, and J. W. Haus: Jpn. J. Appl. Phys. **38** (1999) L157.
6) K. Inoue, M. Wada, K. Sakoda, M. Hayashi, T. Fukushima, and A. Yamanaka: Phys. Rev. B **53** (1996) 1010.
7) H.-B. Lin, R. J. Tonucci, and A. J. Campillo: Appl. Phys. Lett. **68** (1996) 2927.
8) F. Du, Y. Q. Lu, and S. T. Wu: Appl. Phys. Lett. **85** (2004) 2181.
9) M. Notomi, T. Tamamura, Y. Ohtera, O. Hanaizumi, and S. Kawakami: Phys. Rev. B **61** (2000) 7165.
10) S. Shimada, S. Hirano, and M. Kuwabara: Jpn. J. Appl. Phys. **42** (2003) 6721.
11) Y. Watanabe, N. Yamamoto, and K. Komori: Jpn. J. Appl. Phys. **43** (2004) 2015.
12) M. Agio and L. C. Andreani: Phys. Rev. B **61** (2000) 15519.
13) C. Goffaux and J. P. Vigneron: Phys. Rev. B **64** (2001) 075118.
14) R. Hillerbrand, W. Hergert, and W. Harms: Phys. Status Solidi B **217** (2000) 981.
15) K. P. Chang and S. L. Yang: J. Appl. Phys. **100** (2006) 073104.
16) C. M. Anderson and K. P. Giapis: Phys. Rev. Lett. **77** (1996) 2949.
17) D. Cassagne, C. Jouanin, and D. Bertho: Phys. Rev. B **53** (1996) 7134.
18) J. D. Joannopouls, R. D. Mead, and J. N. Winn: *Photonic Crystals, Modeling the Flow of Light* (Princeton University Press, Princeton, NJ, 1995).
19) N. Susa: J. Appl. Phys. **91** (2002) 3501.
20) M. Qiu and S. He: J. Opt. Soc. Am. B **17** (2000) 1027.
21) C. S. Kee, J. E. Kim, and H. Y. Park: Phys. Rev. E **56** (1997) R6291.
22) R. Wang, X. H. Wang, B. Y. Gu, and G. Z. Yang: J. Appl. Phys. **90** (2001) 4307.
23) L. Shi, F. Zhang, C. Li, and X. Jiang: Opt. Commun. **267** (2006) 402.
24) J. C. Slater and G. F. Koster: Phys. Rev. **94** (1954) 1498.
25) N. W. Ashcroft and N. D. Mermin: *Solid State Physics* (Saunders College, Philadelphia, PA, 1976).